Verifying Microexhausts with Schlieren Imaging

Ville Lekholm[1], Kristoffer Palmer[1], Håkan Johansson[2], Pelle Rangsten[2] and Greger Thornell[1]
[1)]Ångström Space Technology Centre, Uppsala University, Uppsala, Sweden
[2)]NanoSpace, Uppsala, Sweden
E-mail: ville.lekholm@angstrom.uu.se

Schlieren imaging is a method to visualize differences in refractive index within a medium. It is an inexpensive, yet powerful and straightforward tool, for sensitive and high-resolution visualization of gas flows. Here, heated cold gas microthrusters were studied with schlieren imaging techniques. The thruster chips are manufactured using MEMS technology, and measure 22×22×0.85 mm. The nozzles are approximately 20 µm wide at the throat, and 350 µm wide at the exit. Through these studies, verification and direct visualization of the functionality of the thrusters were possible. At atmospheric pressure, slipping of the exhaust was observed, due to the severe overexpansion of the nozzle. In vacuum, the nozzle was underexpanded, and the flow was seen to be supersonic. There was a measurable change in the exhaust with heaters activated. It was also shown that the method can be used to detect leaks, making it a valuable, quick, safe, and inexpensive aid in quality control of the thrusters.

Introduction

During their missions, spacecraft generally need some type of on-board propulsion system [1]. The size and mass of the satellite, as well as the desired maneuvers will determine what type of thrusters are required, and how much fuel is needed for the mission. The desire to reduce the mass of the spacecraft, while maintaining attitude control, is driving the development of very small and low-thrust propulsion systems [2]. Low-thrust propulsion systems are also key components in missions with larger spacecraft, where extremely accurate attitude adjustments are required, such as the LISA [3] and Darwin [4] missions. This renders microelectromechanical systems (MEMS) devices attractive [5].

In this report, MEMS-based heated cold gas thrusters from the company Nanospace [6] are studied. The microthrusters are fabricated using lithographic patterning of silicon wafers [7], followed by deep reactive ion etching (DRIE) [8]. MEMS technology not only allows for miniaturization of the components themselves, but also for integration with other components [1]. Furthermore, DRIE results in smooth side walls, making it particularly well suited for micronozzles [9], see Figure 1.

In the stagnation chamber, heaters are embedded to heat the gas and thereby increase the pressure in the nozzle throat. The pressure of the gas in the nozzle throat determines the specific impulse, and hence the efficiency of the thruster.

Fabrication of the nozzle using DRIE is not entirely without drawbacks, as it is only possible to etch 2.5-dimensional or quasi 3-D structures, thereby sacrificing optimal form for size. This means that the compression and expansion phases of the jet propellant will suffer from asymmetry. Furthermore, the miniaturization itself may lead to increased viscous losses and other scaling effects that could severely affect performance [2]. It is therefore of interest to determine if, and to what extent, this design compromise will affect the behavior of the exhaust. With these aims, both near and far field exhaust behavior at different flow speeds, ambient pressures, and gas temperatures were investigated in a lens-based schlieren system.

Theory

One way to visualize the gas exhaust, is to use the fact that not only is the gas exiting the nozzle different from the surrounding medium by composition, it is also at different temperature and pressure, and can generally be seen through differences in the refractive index, n_D. All that is required, is fairly collimated light passing through the disturbance and casting a shadow on a screen. This method is called *shadowgraphing*. A related, but more sophisticated technique, is the *schlieren* method. In its simplest embodiment, a second lens – the schlieren lens – is placed after the disturbance to focus the collimated beam onto a *cut-off*, while simultaneously focusing an image of the disturbance onto a screen or imaging device. For many applications, a razor blade will serve very well as a cut-off.

The purpose of the cut-off is to increase contrast in the image. In theory, the schlieren lens will focus the light onto a single point, but, in practice, there will be a focused image of the light source. The cut-off can be moved to block the light to varying degrees, allowing light refracted away from the cut-off to pass unobstructed, but blocking light refracted into the cut-off completely. The schlieren image can then be projected onto a screen directly, or, using a focusing lens, to an imaging device or a screen of desired size. The cut-off needs to be adjustable with high precision to control the background illumination, as this relates to the sensitivity and measuring range of the apparatus [10]. The cut-off can, in the case of the razor blade, be rotated around the optical axis of the set-up to visualize disturbances in different directions.

In general, the light source will be too large for adequate collimation, which will result in poor image quality and sensitivity [10]. To improve this, a condensing

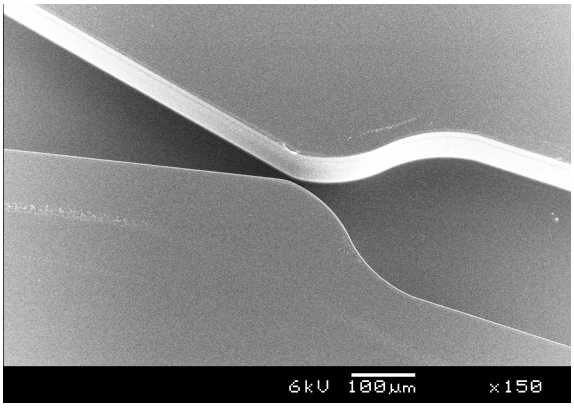

Figure 1: Image of a micronozzle manufactured using DRIE. Gas is exhausted to the left.

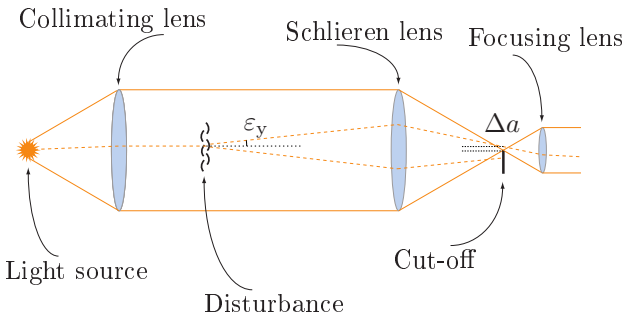

Figure 2: Simplified schlieren set-up, with ε_y denoting angle of refraction of a light ray, and Δa the resulting displacement at the cut-off.

lens is often used to focus the light onto an aperture or slit, which will then emulate a pointlike (aperture), or extended pointlike (slit) light source. By using variable apertures or slits, the degree of collimation can be adjusted depending on the disturbance to be visualized. A schematic of the basic setup can be seen in Figure 2. It is desirable to have the largest possible focal length for both the collimating lens and the schlieren lens.

Materials and Methods

Schlieren set-up

For this study, viewing areas of only a few centimeters were necessary, and an optical table was available of sufficient size to incorporate an in-line lens schlieren system with very little compromise regarding choice of focal lengths and f-numbers. The light source used for this study was a 1 kW quartz-tungsten-halogen (QTH) lamp (Newport Oriel 6317) with a water-cooled infrared filter (Newport Liquid Filter 6127), and a high quality photographic ultra violet filter (Hoya UV(0) HMC) mounted in series directly on the focusing barrel. Due to the extent of the lamp filament (5×18 mm), the beam from the lamp was only quasi-collimated, and the small relative aperture of the condensing lens in the lamp housing [11] caused rather severe spherical aberration. In order to improve collimation, a 300 mm $f/5.9$ lens was used to focus the beam from the lamp onto a variable slit (Thorlabs VS100/M), mounted on a translation stage (2×Thorlabs PT1/M) for X-Y adjustment. After the slit, an identical lens, mounted on a single translation stage (Thorlabs PT1/M) for X adjustment, then collimated the light through the test area.

For studies in vacuum, a small cylindrical vacuum chamber with an inner diameter of 15 cm, and an internal height of 12.5 cm, was constructed. The bottom plate was designed to include an electrical feedthrough with an external female 25-pin RS232 connector, as well as two 1/16" NPT connections, one for the vacuum pump, and one for the propellant gas (via a 15 µm filter (Swagelok SS-4F-15) and a quick release valve). The chamber had two opposing 40 mm KF flanges fitted with sight glasses of high quality borosilicate glass. A mechanical manometer on top of the chamber enabled pressure read-out. When performing tests in vacuum, the chamber was evacuated using an ULVAC G-5D oil rotary pump.

The schlieren lens is a 400 mm $f/7.9$ achromatic doublet (Thorlabs AC508-400-A1), focusing the light to the schlieren cut-off, while simultaneously focusing the disturbance to the focusing lens (see Figure 3).

In this set-up a razor blade cut-off was used. This was mounted on an X-Y-positioning fixture, ensuring accurate positioning of the cut-off in the focal point, as well as enabling very precise lateral adjustment. A cut-off of 95-99% was used to maximize sensitivity and contrast of the images, while maintaining a full measuring range.

Imaging was achieved with a Sony α350 digital SLR, and a Canon 50 mm $f/1.8$ FD lens mounted on a bellows, to enable variable magnification. At the maximum magnification, the lens and bellows combination magnified the live image approximately 3.6 times, imaging an area of 4.5×7 mm. The magnification in the far field images is adapted depending on the orientation of the jet in relation to the camera.

The entire set-up, Figure 3, was put on a 3×1.5 m optical table top (Melles Griot 07 OTR 517).

Test Series

The thruster chips studied, were mounted in an aluminum fixture which secured the chip while at the same time ensuring power supply and gas connection, Figure 4. The fixture was mounted to the base of the vacuum chamber via a bracket. The gas connection was accomplished by a 1/8" NPT elbow to 1/16" Swagelok tube connector (Swagelok part SS-100-2-2) at the bottom of the fixture, opposite to the nozzle. Electrical probes for contact with the heaters were connected to two 9-pin RS232 female connectors, one on each side of the fixture. A groove was milled from the top edge of the fixture down to the edge of the thruster chip to enable viewing of the exhaust gas from the nozzle.

3 thrusters were used for this study [6]. All were designed to use xenon gas as propellant.

Studies at atmospheric pressure. Initial experiments were conducted at atmospheric pressure in order to better predict and understand the behavior of the thrusters in later tests. These studies were also to verify the function and optimize the use of the schlieren set-up with regard to thruster position, and establish cut-off

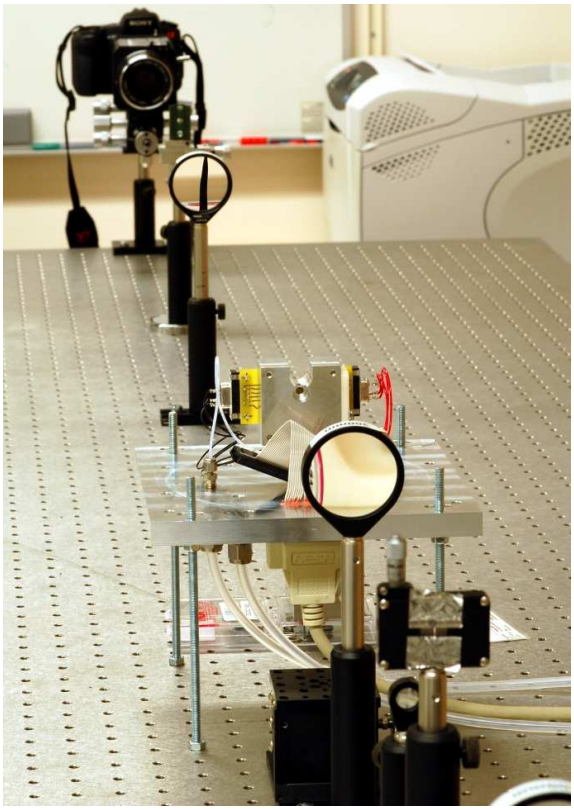

Figure 3: Final setup. From bottom right to top left: variable slit, collimating lens, test area, schlieren lens, cut-off, and camera with mounted lens and bellows.

percentage for optimum image quality. Tests with and without the vacuum chamber in place were also conducted in order to determine any effects the vacuum chamber and sight glasses could have on the images.

- Helium, nitrogen and xenon gases were used
- Flow was studied with cut-off parallel to, or perpendicular to flow

The jet exhausts of the thrusters were photographed with inlet pressures ranging from 0.5 to 3.5 bar (gauge pressure) in steps of 0.5 bar. Images were acquired with longer and shorter exposure times – longer (1/60 s, ISO 100) to minimize sensor noise while maintaining exposure values, shorter (1/1000 s, ISO 1600) to enable more time resolved visualization of the behavior of the gas.

Studies in vacuum. The thruster chips used in the atmospheric tests were again studied, but this time in low vacuum (approximately 3 kPa). As in the atmospheric tests, the chips were tested with several different gases (helium, nitrogen, and xenon) at different inlet pressures, this time starting at -0.5 bar gauge pressure, and ending at 3.5 bar in steps of 0.5 bar. These tests were repeated with the thruster chip placed horizontally and vertically in order to study the exhaust jet with the cut-off parallel to, as well as perpendicular to, the flow.

Studies with heaters activated. In order to fully examine the behavior of the thrusters, studies were also conducted with the heaters activated. When activated, heater 1 (closest to the nozzle) was connected separately to 13.6 V at 71.9 mA (0.98 W), whereas heaters

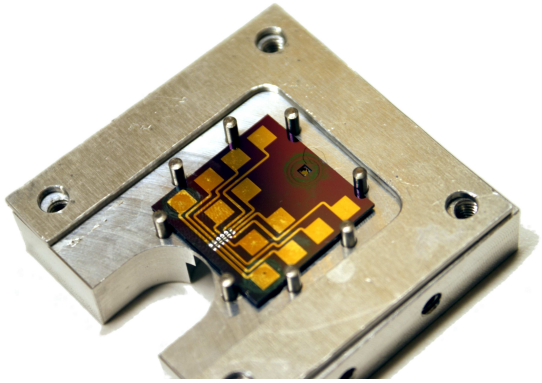

Figure 4: Thruster chip (22×22 mm) in opened fixture. The U-shaped spacer and eight alignment pins surround the silicon chip. The thruster exhausts into the milled groove in the bottom left of the picture. Here, 12 connector pads are used to drive the heaters.

2 and 3 were connected in parallel to 13.6 V at 204 mA (2.77 W total).

Tests were conducted with: no heaters active, only the heater closest to the nozzle active, and all heaters active. These tests were conducted at both atmospheric pressure and in vacuum (3 kPa). Images were captured at 3.5 bar inlet gauge pressure at atmospheric pressure, and 3 bar inlet gauge pressure in vacuum.

Data processing

The images acquired were 4592×3056 pixel RGB channel JPEG images. As only the intensity data was of interest when using the a razor blade cut-off, the three color channels were simply added together to create a gray-scale image one third of the original file size. To minimize dynamic noise, e.g. dust particles in the beam, the median of several images was calculated. In order to eliminate as much of the static noise as possible, a reference image without disturbances was subtracted from the signal images. This compensated for uneven background illumination, and dust particles on the lenses, mirrors, sight glasses, etc. Finally, the image was adjusted with respect to brightness and contrast.

Results

Test series

Studies at atmospheric pressure. The results from thruster chip #1 with helium gas at 1, 2, and 3.5 bar, can be seen in Figures 5a, b and c, respectively, depicting the jet flow with cut-off parallel to the jet exhaust. A leak that made imaging at atmospheric pressure difficult was discovered, wherefore the tests were repeated with thruster #2. The leakage can be seen as unevenness of the background illumination, particularly at the highest pressure.

At low inlet pressure, the exhaust jet is seen to stick to one side. As the pressure increases slightly, the jet straightens out, and narrows, Figure 5.

With the cut-off perpendicular to the flow, the edges of the exhaust were less distinct, but instead, turbulence in the flow could be visualized. The flow was very

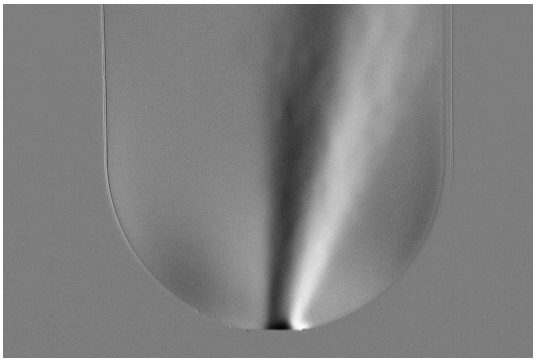

(a)

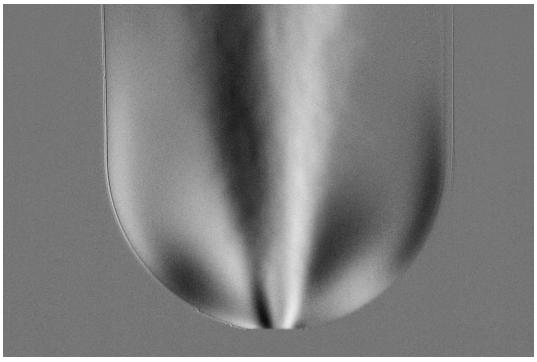

(b)

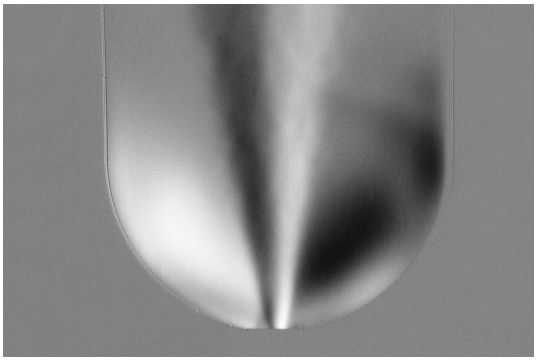

(c)

Figure 5: Exhaust from thruster chip #1, helium gas, cut-off parallel to jet. (a) 1 bar gauge pressure. (b) 2 bar gauge pressure. (c) 3.5 bar gauge pressure. The lighter and darker areas of the background are due to leaking gas. Field of view is 21×14 mm.

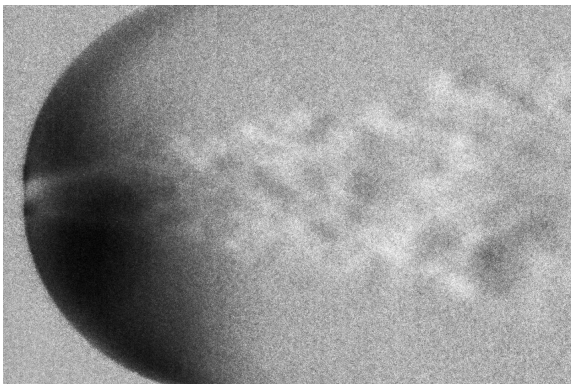

Figure 6: Exhaust from thruster chip #1 photographed with cut-off perpendicular to flow, 1/1000 s exposure time, ISO 1600. Notice the darker area close to the nozzle due to leakage. Field of view is 21×14 mm.

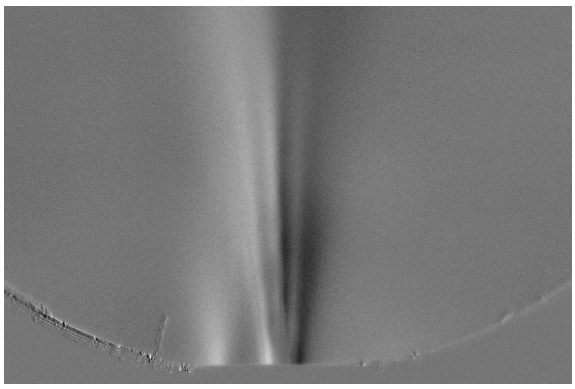

Figure 7: Exhaust from thruster chip #1 in vacuum, cut-off parallel to exhaust jet. The lighter area to the left of the jet is due to leaking gas. Field of view is 7×4.5 mm.

fast, and the details, unless stationary, were generally lost due to motion blur. At atmospheric pressure, the speed of the exhausted gas was still low enough, that shorter exposure times did resolve more detail. Because of the higher ISO required to maintain the same exposure value, more noise was introduced. In Figure 6, the exhaust jet from thruster chip #1 is shown, photographed with the cut-off perpendicular to the flow.

The results were the same regardless of the gas used, but the visibility of the exhaust was related to the difference in refractive index of the gas from the thruster, and the surrounding medium. Here, i.e. in air, xenon gas was easiest to visualize, closely followed by helium. Nitrogen was very difficult to distinguish, due to its refractive index difference of only 6×10^{-6}, compared to the Δn_D of xenon of 4×10^{-4} and helium of 2.6×10^{-4}.

Studies in vacuum. In vacuum, the visibility of the different gases was different from that at atmospheric pressure, as vacuum has an index of refraction defined as 1. This meant that, again, xenon was easiest to see with a Δn_D of 7×10^{-4}, but this time followed by nitrogen with a refractive index difference of 3×10^{-4}. Helium was difficult to visualize due to a Δn_D of 3.5×10^{-5}. The studies in vacuum, using chip #1, better revealed the source of the leak discovered in the atmospheric tests. In Figure 7, the leak can be seen as a lighter area to the left of, and separate from, the main jet.

The tests at step-wise increased pressure show a behavior significantly different from that at atmospheric pressure. The gas jet was straight and narrow even at the lowest pressure, and then became increasingly distinct as the inlet pressure increased. The erratic behavior of the jet at atmospheric pressure was not observed. An image of thruster chip #2 at 3 bar gauge pressure can be seen in Figure 8a. No apparent differences were noticed with shorter exposure times.

When visualizing the jet with the cut-off perpendicular to the flow, the situation was again different. The pressure differences in the jet now appeared to be stationary, and could easily be photographed even with relatively long exposure times. Notice the cross pattern in the jet in Figure 8b. The picture is an image of the exhaust from thruster chip #2 at 3 bar gauge pressure

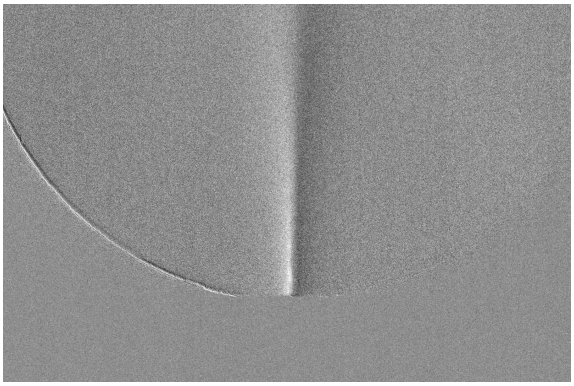

(a)

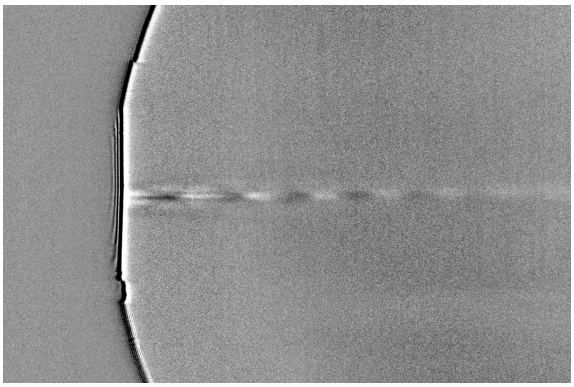

(b)

Figure 8: Image of jet exhaust from thruster chip #2 in vacuum (a) with cut-off perpendicular to flow. Field of view is 12.5×8.3 mm, (b) with cut-off perpendicular to jet. Field of view is 7×4.5 mm.

xenon in 3 kPa vacuum. The cut-off is perpendicular to the flow.

Studies with heaters activated. At atmospheric pressure, there was a noticeable difference in the sound of the exhaust when the heaters were activated, but no visible difference from the images without heaters active. Figure 9a shows parts of the near-field images from thruster chip #3 at 3 bar gauge pressure at the inlet. Figure 9b-d shows graphs of the intensity of the processed schlieren images along a one-pixel wide horizontal centerline of the jet. The gray line is the intensity, with the uniform gray of the fixture to the left, and the periodic intensity fluctuation of the gas exhaust slowly fading to a nearly smooth line. The red line is a 50 point moving average of the intensity to compensate for some of the noise in the image. From these graphs, the distance between the pressure maxima can be measured, and using the known size of the depicted area, translated to distances. The total length of the graph is approximately 7 mm. A total horizontal resolution of 4592 pixels gives a linear resolution of 660 pixels/mm, or 1.5 µm/pixel. Averaged between three measurements, the distance between the peaks is 0.64 mm with no active heaters, 0.57 mm with one active heater, and 0.54 mm with all heaters active.

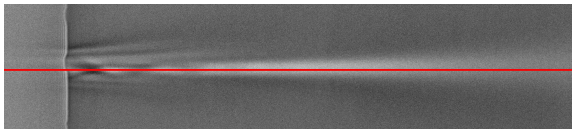

(a)

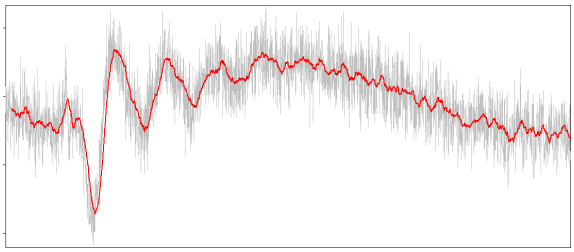

(b)

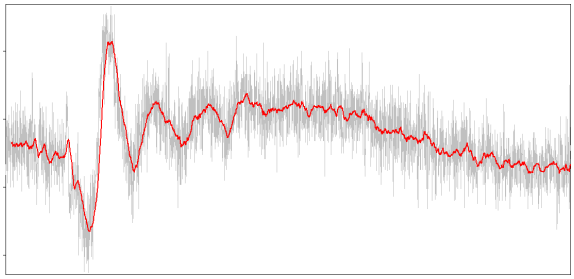

(c)

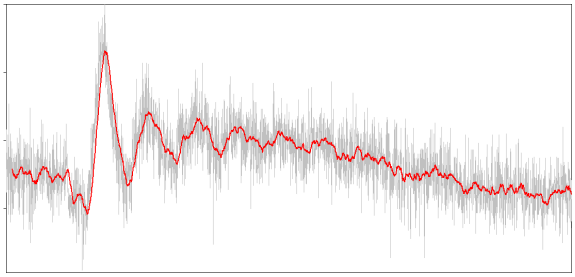

(d)

Figure 9: Intensity graphs of thruster chip #3 at centerline of jet. (a) indicating measurement line. (b) No heaters activated. (c) Heater nearest nozzle active (0.98 W). (d) All three heaters active (3.75 W). Field of view is 7×1.5 mm.

Discussion

Schlieren imaging

With the schlieren setup, almost all of the light is lost in each step along the way: from the lamp itself, via the slit and the cut-off. This means that both a high intensity light source and a sensitive imaging device are important.

The lenses was chosen specifically for optimum performance for these tests. The challenge with schlieren photography is often to maximize field of view at reasonable cost, but here, many of these problems were absent, due to the small field of view necessary. The two lenses could have been exchanged for matched mirrors, saving length, but making alignment more difficult [10]. Furthermore, at this scale, there would be no cost benefit over lenses. Even the lenses used in this study were larger than needed for the final tests, but the difference in cost was negligible, especially when taking into account the increased versatility and ease of setup that the larger lenses permitted.

Neither the light source nor the camera were acquired specifically for this project, but rather for general use. Different equipment could target specific needs, such as low noise, or high-speed capabilities.

In the end, it will be the amount of available light that limits the sensitivity and magnification. Increased sensitivity requires a narrower slit or aperture before the collimating lens, which will reduce the amount of transmitted light. Sensitivity can also be increased by increasing the level of cut-off, reducing the light transmitted to the imaging device even further. Magnification will have the same effect, as a smaller part of the beam will reach the sensor, and the intensity will decrease proportionally to the square of the viewing distance.

If different propellants, smaller gas quantities, or even smaller nozzles are to be studied, upgrades, primarily of the light source, may be necessary. Increasing the magnification on the imaging side by a factor of two with the current equipment will already be pushing the limits, but it is not difficult to find arc discharge lamps capable of over 100 times higher light output after collimation (due to the smaller source). Thus, much higher magnification is absolutely possible.

Test series

While some types of defects can be detected by other means, leakage and anomalies in the jet behavior would likely go unnoticed without visualization of the flow. In order to be able to gain the best possible understanding of the behavior of these microthrusters, the same chip would have needed to be used for all the studies. As these were bread-board chips, some tests were conducted with thruster chips that proved to be unusable for later tests.

Studies at atmospheric pressure. It is obvious that the behavior of the thrusters would be very different at atmospheric ambient pressure and in vacuum. The atmospheric tests gave a very good understanding of the fundamentals of nozzle design, and were a useful aid in predicting the behavior in the subsequent vacuum studies. The studies at atmospheric pressure also provided a suitable transition from preparatory experiments conducted previously to evaluate the schlieren setup. The unpredictable behavior of the jet exhaust observed, should not be the basis of any conclusions regarding performance in their intended environment. The atmospheric studies were also necessary to evaluate the effects of the vacuum chamber.

Important observations concerned the leaks near the nozzle. With thruster chip #1, a leak was noticeable in all images, and clearly visible in Figure 7.

At atmospheric ambient pressure, the jet exhausts all appeared to be turbulent and subsonic.

Studies in vacuum. When the thrusters were studied in vacuum, the behavior was completely different from that at atmospheric ambient pressure. The speed of the gas exhaust was higher, so details were expected to be difficult to distinguish, but this was not the case. It was immediately clear that the strange behavior observed at atmospheric ambient pressure, was simply an indication that the thruster was not operating in its proper environment. In vacuum, the jet exhausts were observed to be supersonic and laminar. The appearance of pressure disks, for example in Figure 8b, confirmed this.

The differences between the appearance of the jets in Figure 7 and Figure 8a could be due to either a difference in design, or the leak near the nozzle causing lower throat pressure or extending to affect the shape of the expansion cone.

The sight glasses of the vacuum chamber were of sufficient quality for schlieren work. However, by their introduction, four additional surfaces that could collect dust were introduced. While this were fairly easily removed, either physically or in postprocessing, this should be an incentive to minimize surfaces in the beam, regardless of their optical quality.

The quality of the chamber, and the capacity of the pump limited the vacuum pressure to around 3 kPa in these studies.

Studies with heaters activated. The difference with and without heating could be observed as a difference in the appearance of the jet exhaust, Figure 9b-d. The image series also shows an increasing degree of asymmetry in the jet exhaust. Whether this is caused by an irregularity in or around the nozzle (either the damage near the nozzle exit, or less visible damages), or by some phenomenon in, or just behind the throat of the nozzle, such as the gas traveling through the heaters, is unknown.

The distance between the pressure nodes in the resulting images can be measured, as the size of the image is known. By these measurements, it is possible to obtain quantitative results, which can be related to heater function.

Conclusions

Schlieren imaging proved to be a powerful technique capable of visualizing very faint phenomena under various conditions and in different media. The set-up is adaptable, and can be designed or modified to suit specific needs.

For optimum performance, some aspects are more important than others.

- A powerful light-source with a small extension, and non-coherent light is needed.
- High quality lenses with the largest possible focal lengths, and small relative apertures are desirable. Preferably $f/8$ or less.
- Sensitive imaging equipment with low noise will increase resolving power.

As these were prototype thrusters, the schlieren technique was particularly useful, as it was able to visualize defects, e.g. leakage, that would likely have gone unnoticed without this method. It was also possible to observe the exhaust behavior at different pressures. The relative ease with which this apparatus is set up, the relatively low cost compared with the manufacturing cost of the thruster chips, and the very low risk acceptance due to the very high total cost of the missions, makes this a very useful method for pre-launch tests of the thrusters.

- Studies either at atmospheric pressure or in vacuum can be used to identify (and locate) leaks in the thrusters.
- Appearance of the jet exhaust in vacuum visualized with cut-off perpendicular to flow can give useful quantitative information about the jet.

In order to incorporate this method as part of the quality control process, a quick release fixture would enable replacement of the thruster chips without affecting focus or adjustment of the schlieren apparatus.

References

[1] Johan Bejhed. *Fluid Microsystems for Micropropulsion Applications in Space*. PhD thesis, Uppsala University, 2006.

[2] Robert L. Bayt. *Analysis, Fabrication and Testing of a MEMS-based Micropropulsion System*. PhD thesis, Massachusetts Institute of Technology, 1999.

[3] John K. Ziemer and Stephen M. Merkowitz. Microthrust propulsion of the LISA mission, in 40th AIAA joint propulsion conference. Fort Lauderdale, Florida, July 12-14 2004.

[4] G. Saccoccia, J. Gonzalez del Amo, and D. Estublier. Electric propulsion: A key technology for space missions in the new millenium. *ESA bulletin*, 2000.

[5] Tor-Arne Grönland, Pelle Rangsten, Martin Nese, and Martin Lang. Miniaturiaztion of components and systems for space using MEMS-technology. *ScienceDirect Acta Astronautica*, 61:228–233, 2007.

[6] Micro propulsion cold gas thrusters phase 3 & 4. ESA contract: 18592/NL/HE. Available from NanoSpace as product "Cold Gas Thruster EM-design".

[7] Marc J. Madou. *Fundamentals of Microfabrication The Science of Miniaturization*. CRC Press, 2002.

[8] J. Köhler, J. Bejhed, H. Kratz, U. Lindberg, K. Hjort, and L. Stenmark. A hybrid cold gas microthruster system for spacecraft. *Sensors and Actuators*, 97-98:587–598, 2002.

[9] A.A. Ayón, R.L. Bayt, and K.S. Breuer. Deep Reactive Ion Etching: a promising technology for micro- and nanosatellites. *Smart Materials and Structures*, 10:1135–1144, 2001.

[10] G.S. Settles. *Schlieren and Shadowgraph Techniques*. Springer-Verlag, Berlin, 2001.

[11] *Newport Oriel Product Line, 1000W QTH Lamp Housing Models 66861, 66885 & 66886 User Manual*.